2009

Ion channels underlying stimulus-exocytosis coupling and its cell-to-cell heterogeneity in β-cells of transplantable porcine islets of Langerhans

Amelia M. Silva
Washington University School of Medicine in St. Louis

Adam S. Dickey
Washington University School of Medicine in St. Louis

David W. Barnett
Washington University School of Medicine in St. Louis

Stanley Misler
Washington University School of Medicine in St. Louis

[Channels 3:2, 91-100; March/April 2009]; ©2009 Landes Bioscience

Research Paper

Ion channels underlying stimulus-exocytosis coupling and its cell-to-cell heterogeneity in β-cells of transplantable porcine islets of Langerhans

Amelia M. Silva,† Adam S. Dickey,‡ David W. Barnett§ and Stanley Misler*

Departments of Internal Medicine and Cell Biology/Physiology; Washington University Medical Center; Saint Louis, MO USA

†Current address: Department of Biology and Environment; CITAB; University of Trás-os-Montes e Alto Douro; Vila Real, Portugal; ‡Current address: Medical Scientist Training Program; University of Chicago Medical Center; Chicago, IL USA; §Current address: Department of Biomedical Engineering; Saint Louis University; St. Louis, MO USA

Abbreviations: $[cAMP]_i$, cytosolic cAMP concentration; PSS, physiological saline solution; $[Ca^{2+}]_i$, cytosolic $[Ca^{2+}]$; QREs, amperometrically measured quantal release events; ΔC_m, membrane capacitance change

Key words: stimulus-exocytosis coupling in β-cells, ion channels in β-cells, β-cell electrical activity, β-cell heterogeneity, phasic and tonic exocytosis

Given the growing interest in porcine islets as model tissue for studying the pathogenesis of human diabetes mellitus and its treatment by transplantation, we investigated stimulus-exocytosis coupling in single porcine β-cells using patch clamp electrophysiology, Ca^{2+} imaging, capacitance tracking and amperometry. We establish that porcine β-cells display several features prominently seen in β-cells from human islets of Langerhans. These include: (i) wide heterogeneity of electrical responsiveness to glucose; (ii) dependence of action potential activity on voltage-dependent Na^+ as well as high voltage activated Ca^{2+} current; (iii) heterogeneity of time course of depolarization-evoked insulin granule exocytosis; and (iv) the dependence of vigorous single cell electrical activity and insulin granule exocytosis on the presence of agents that enhance cytosolic cAMP concentration. These findings promote the usefulness of porcine β-cells as a model for studying β-cell function in large mammals, including humans, as well as an appropriate source of tissue for xenotransplantation.

Introduction

Currently, strains of pigs are being developed as both (i) model systems for understanding the long-term interactions of genes, diet and other environmental factors in the development of both Type 1 and Type 2 diabetes mellitus[1,2] and (ii) sources of antigenically homogeneous and relatively pathogen free islets to permit xenotransplantation to treat diabetes mellitus in humans.[3,4] However, a general understanding of stimulus-secretion coupling in porcine islet cells is not yet available because detailed single cell physiological studies have not been performed. To remedy this deficiency, as well as determine whether some unusual features of β-cells of human islets, usual derived from metabolically compromised life-supported cadavers, are generalized to larger mammals, we have applied a variety of single cell assays, to single freshly isolated porcine β-cells to study their process of stimulus-exocytosis coupling in response to glucose- and voltage clamp-induced excitation.

Using patch-clamp electrophysiology, fluorescence imaging of cytosolic $[Ca^{2+}]$ ($[Ca^{2+}]_i$), and capacitance and amperometry assays to monitor exocytosis, we have established that porcine β-cells display the basic paradigm of stimulus-exocytosis coupling characteristic of rodents,[5] namely glucose metabolism → closure of ATP sensitive K^+ channels → cell depolarization → activation of voltage dependent Ca^{2+} channels → Ca^{2+} entry-triggered exocytosis of insulin granules. In addition, porcine β-cells display features prominently seen in human β-cells,[6-9] though also seen to varying degrees in rodent[10-12] as well as canine[13,14] β-cells. The latter include (i) wide heterogeneity of electrical responsiveness to glucose, likely reflecting cell to cell heterogeneity in the glucose uptake and metabolism; (ii) dependence of action potential activity on voltage-dependent Na^+ as well as high voltage activated (HVA) Ca^{2+} current; (iii) heterogeneity of time course of depolarization-evoked insulin granule exocytosis, and (iv) the dependence of vigorous single cell electrical activity and insulin granule exocytosis on the presence of agents that enhance cytosolic cAMP, including glucagon, and the incretin glucagon-like peptide-1.

These findings present us with a detailed outline of stimulus-exocytosis coupling in porcine β-cells as well as confirm, in freshly isolated cells, features of stimulus-exocytosis coupling prominently displayed by human β-cells, which however are generally only available by harvesting from semi-ischemic cadaver-donor sources.

*Correspondence to: Stanley Misler; Box 8126/Renal Division; Department of Internal Medicine; Washington University Medical Center; St. Louis, MO 63110 USA; Tel.: 314.454.7719; Fax: 314.454.5126; Email:smisler@dom.wustl.edu

Submitted: 11/17/08; Revised: 01/15/09; Accepted: 01/16/09

Previously published online as a *Channels* E-publication:
http://www.landesbioscience.com/journals/channels/article/7865

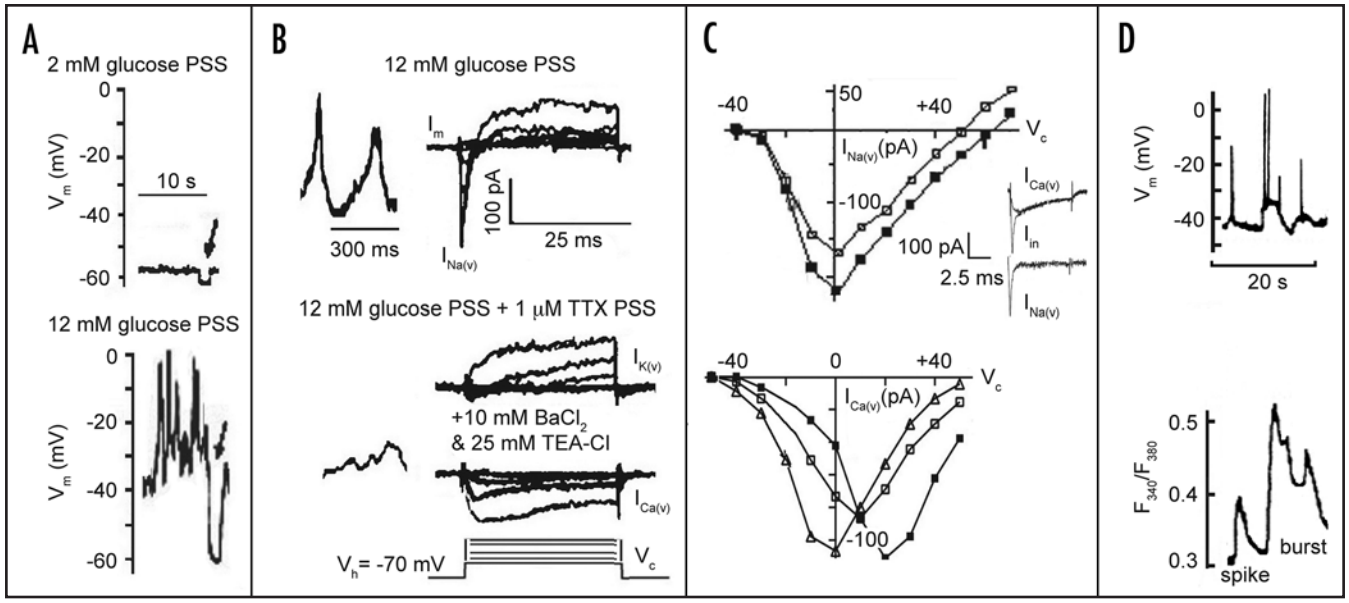

Figure 1. Single cell perforated-patch recording of stimulus-depolarization coupling in porcine β-cells. (A) shows recordings of membrane voltage (V_m), made in current-clamp mode from a β-cell exposed to a PSS containing 2 mM glucose (upper trace) and again 5 min after changing the bath to a PSS containing 12 mM glucose (bottom trace). Hyperpolarizing test current pulses of -5 pA were applied at intervals (see arrows) to ascertain membrane conductance, G_m. In response to increased bath glucose note the membrane depolarization, increased hyperpolarizing response to test pulse, indicating decreased G_m, as well as the development of complex action potentials (APs). (B) presents alternating recording of V_m and membrane currents (I_m), under voltage clamp conditions, first in PSS with 12 mM glucose, before (upper traces) and then after the addition of 1 μM TTX (lower traces). I_ms were evoked by depolarizing step pulses applied in random sequence at 0.2 Hz from a holding potential (V_h) of -70 mV to clamping potentials (V_c) of -40 to 0 mV. Note that addition of TTX blocks fast inward current, tentatively identified as $I_{Na(V)}$, while leaving intact the outward current, tentatively identified as a voltage dependent K current $I_{K(V)}$. Subsequent isosmotic replacement of NaCl with 10 mM $BaCl_2$ + 25 mM TEA reveals a smaller, slowly activating inward current tentatively identified as a voltage dependent, L-type Ca current, $I_{Ca(L)}$. (C) presents more definitive voltage clamp identifications of $I_{Na(V)}$ and $I_{Ca(L)}$. Top, $I_{Na(V)}$ vs. V_c obtained on depolarizing from V_h = -70 mV to the indicated V_c in two different ionic conditions: (i) in standard PSS (containing 134 mM Na^+), where the current peaked at ~0 mV and reversed at ~+62 mV (■); and (ii) in partial N-methylglucamine Cl-substituted PSS (containing 82 mM Na^+) where the current peaked at ~0 mV but reversed at ~+50 mV (□). As presented in the inset traces, whole cell $I_{Na(V)}$ was identified as a difference current, namely between whole-cell inward current recorded from cells patched with a pipette containing a Cs^+-IS solution prior to, and then after, addition of 1 μM TTX to bath. The residual current was taken as $I_{Ca(v)}$. Bottom, $I_{Ca(v)}$ vs. V_c obtained on depolarizing from V_h = -70 mV to the indicated V_c in three different PSSs. In a standard PSS containing 2 mM $CaCl_2$ (□), current peaked at ~10 mV and was extrapolated to reverse at ~+60 mV; in a modified PSS containing 5 mM $CaCl_2$ (■), the current peaked at 20 mV and was extrapolated to reverse at ~positive to +70 mV; and in a modified PSS containing 2 mM $BaCl_2$ (denoted by open triangles), the current peaked at 0 mV and was extrapolated to reverse at ~positive to +55 mV. (D) presents simultaneous recording of V_m (*upper traces*) and global cytosolic [Ca^{2+}], ([Ca^{2+}]$_i$), (*lower traces*) during exposure to 12 mM glucose. Note single APs evoke small transient rises in [Ca^{2+}]$_i$ denoted as spikes, while short trains of APs (here 2 APs) evoke large and longer transients denoted as bursts.

Results

Ionic currents underlying stimulus-depolarization coupling in single porcine β-cells. Figure 1 examines the roles of closure of background ATP-sensitive K (K^+_{ATP}) channels and subsequent opening of voltage dependent Na^+, K^+ and Ca^{2+} channels in generating glucose-induced depolarization and electrical activity from single porcine β-cells monitored in the perforated patch whole cell recording configuration. Note in *Panel A,* the membrane potential *(V_m)* of the cell bathed in a PSS containing 2 mM glucose and patched with a pipette containing K^+(IS) was stable at ~-55 mV (range -60 to -52 mV, in six cells). From the membrane hyperpolarization (nearly 10 mV) evoked by a test inward current pulse of -5 pA, the resting membrane conductance (G_m) was calculated at the measured access resistance (R_a) as 1085 pS, using the equation

$$G_m = I\,(\Delta V_m - IR_a)$$

(range 725 to 1,150 pS in 6 cells). After 5-minute exposure to [glucose]$_o$ = 12 mM, in all of the cells monitored V_m depolarized to -40 to -35 mV and G_m declined to 200 to 150 pS; thereafter the cells displayed irregular bursts of action potentials, with peak voltages between -20 and +5 mV. However, 2 min after further addition of 1.5 mM NaN_3, an inhibitor of mitochondrial oxidative metabolism, the cells hyperpolarized to -65 mV, G_m increased to 3,000 pS and all electrical activity ceased (data not shown). The simultaneous depolarization of V_m with a decrease in G_m on addition of glucose, followed by the rapidly reversible hyperpolarization with an increase in G_m on transient addition of NaN_3, essentially identifies the underlying conductance change as that of closure of background K^+ channels, of which K^+_{ATP} is most the plentiful and metabolically responsive in most β-cells thus far examined.

As shown in *panel B*, in porcine β-cells cells monitored under perforated patch conditions it was possible to switch alternately from current-clamp to voltage-clamp recording to dissect and

tentatively identify, by voltage pulse and pharmacological maneuvers, the membrane currents underlying the glucose-induced action potential activity. In voltage-clamp mode, depolarizations from a holding potential of -70 mV to clamping potentials (V_cs) between -30 and 0 mV revealed early inward current, peaking between 0.5 and 1.5 ms after the step depolarization; this was followed by delayed, sustained outward current best seen at V_cs positive to -20 mV. After addition of tetrodotoxin (TTX), at a concentration of 1 μM, action potentials were no longer visible in the current-clamp mode and the inward current was no longer visible in the voltage-clamp mode, tentatively identifying this current as a voltage-dependent Na^+ current, $I_{Na(V)}$. Subsequently, replacement of the TTX-containing PSS with one containing an additional 10 mM barium chloride (Ba^{2+}, a divalent cation highly conductive through Ca^{2+} channels) and 25 mM tetraethylammonium chloride (TEA, a potent blocker of voltage-dependent K^+ channels) produced two effects. *First*, it nearly abolished the outward current, hence tentatively identifying it as a likely voltage-dependent K^+ current, $I_{K(V)}$; *second*, it revealed a slowly developing, poorly inactivating inward current, tentatively identified as likely Ca^{2+} current, $I_{Ca(V)}$. Very similar currents were seen in each of the six cells examined in this way suggesting that regardless of their apparent heterogeneity of response to glucose, porcine β-cells have very similar $I_{Na(V)}$, $I_{Ca(V)}$ and $I_{K(V)}$ that underlie action potential electrogenesis.

Panel *C* presents a more definitive identification and quantitation of $I_{Na(V)}$ and $I_{Ca(V)}$ performed on another set of cells. $I_{Na(V)}$ was identified as the difference between total inward current under control conditions and the inward current remaining after application of 1 μM TTX; it closely resembled that in human β-cells. *First*, it peaked at +5 mV; *second*, its reversal potential showed a Nernstian dependence on $[Na^+]_o$, shifting negatively by 12 mV on reduction of bath $[Na^+]$ concentration from 134 mM to 82 mM); and *third*, it was 50% activated at +15 mV and 50% inactivated after a pre-pulse (V_{hold}) of ~-45 mV (see Fig. legend and Supplementary Fig. 2 for details). Current density, measured at +5 mV, averaged -35.4 ± 8.35 pA/pF in porcine β-cells, as compared with values of -30.3 ± 6.25 pA/pF recorded from human β-cells.[23] In contrast, $I_{Ca(V)}$, identified as the residual current after TTX blockade, had a high threshold for activation (~-25 mV) and slow inactivation, peaked at +10 mV with a mean magnitude of 20.5 ± 4.63 pA/pF; its peak amplitude increased on raising $[Ca^{2+}]_o$ to 5 mM or on mole-for-mole replacement of $CaCl_2$ with $BaCl_2$. Hence $I_{Ca(V)}$ strongly resembled the high voltage activated Ca^{2+} current we have previously recorded from rat and dog β-cells under identical conditions.[14] However, unlike the case in human β-cells, no low threshold (T-type) Ca^{2+} current, activated at V_c between -50 and -40 mV, was detected. In several cell-attached patch recordings performed in the presence of an external solution containing near isotonic $BaCl_2$, the only variety of unitary Ca channel identified had a γ_s = 22 pS, typical of L-type Ca^{2+} channels. (see Supplementary Fig. 2).

Panel D presents data from current clamped porcine β-cells previously loaded with Fura-2 whose membrane voltage and ratiometric changes in fluoresecence were simultaneously monitoring. Note that single action potentials evoke modest spike-like increases in the fluorescence ratio, lasting 5 s and estimated to raise cytosolic $[Ca^{2+}]$ by 100–150 nM, while brief trains of 2–4 action potentials evoke more substantial burst-like increases in the fluorescence ratio, lasting up to 20 s and estimated to raise cytosolic $[Ca^{2+}]$ by 200–250 nM.

Depolarization-exocytosis coupling in single porcine β-cells. In single β-cells of rodent, human and canine islets, trains of action potentials and sustained depolarizations result in bouts of exocytosis measured in two ways: (i) as rapid increases in plasma membrane surface area, tracked as increases in capacitance (C_m) of the entire plasma membrane under voltage clamped conditions;[24,25] and (ii) as quantized release of serotonin (5-HT), an oxidizable false transmitter selectively taken up and stored in insulin granules of β-cells and tracked by surface oxidation at the tip of 5 to 8 μm diameter carbon fiber electrode positioned over a limited surface area (amperometry).[21,26,27] Figure 2, which examines the coupling of exocytosis, measured by single cell amperometry and/or capacitance, to electrical activity and sustained membrane depolarization in single porcine β-cells, demonstrates the critical role of Ca^{2+} entry in this coupling as well as the similarity of the time courses of exocytosis as monitored by both assays.

In Panel A, at a porcine β-cell current-clamp electrophysiology was combined with amperometry to produce a train of action potentials, at a frequency of 2 to 5 Hz, in response to continuous 10 s depolarizations and thereby trigger quantal release. In this experiment, representative of a series of 3, when the amperometric electrode, was held at V_{amp} = +650 mV, a voltage where surface oxidation of serotonin is maximal, quantal release events (QREs) commenced roughly midway through the action potential trains. In contrast, QREs were never seen (i) when trains of APs were evoked at V_{amp} = +400 mV (or +900 mV, not shown), voltages at which 5-HT is hardly oxidized, or (ii) when $[Ca^{2+}]_o$ was reduced to 0.1 mM, a concentration at which Ca^{2+} entry through voltage-dependent Ca^{2+} channels is minimal. Assuming that each event represents the simultaneous oxidation of molecules of a single chemical species, 5-HT, and that 4 electrons are liberated by oxidation of a 5-HT molecule,[28] then the average charge transfer associated with a QRE equals that expected from the oxidation of 2.0 x 10^5 5-HT molecules. Such quantities of transmitter are not found in small diameter "synaptic-type" vesicles, but are easily accommodated by the 200 to 300 nm diameter dense core granules of β-cells.[29]

In Figure 2B, recording of whole cell Ca^{2+} current was combined with cytosolic Ca^{2+} imaging and C_m recording in a voltage clamped, Fura-2 loaded cell. It demonstrates the steep dependence of a single cell exocytosis on the quantity of voltage-dependent Ca^{2+}-entry through the high voltage activated Ca channels. Note that a train of five 200 ms depolarization from -70 to +5 mV, which produced large bursts of Ca entry (Q_{Ca} = integrated Ca^{2+} entry during the depolarizing pulse) and major increases in global cytosolic Ca^{2+}, resulted in a readily detectable increase in C_m. In contrast, a train of five 200 ms depolarization from -70 to -25 or +40 mV, each of which provoked ~¼ the Q_{Ca} seen at +5 mV, resulted in barely measurable C_m increases. At depolarizations to

+5 mV, exocytosis remained robust and highly reproducible, so that for trains of repeated (up to 5) ten 200 ms depolarizations, delivered at intervals of >90 s, Ca^{2+} entries, increases in global cytosolic Ca^{2+}, and increases in C_m varied by less than 10%.

Lastly, *Panel C*, compares the time courses of depolarization-evoked exocytosis, measured simultaneously by amperometric and capacitance recording, from porcine β-cell triggered by a train of depolarizing pulses (from -70 to +5 mV) and displaying a complex time course of exocytosis. In this cell, where endocytosis, monitored as the post train recovery of C_m, was very slow, the graph on the left presents evidence that the amplitudes of the C_m steps seen immediately after the depolarization tracked the intensity of the QRE burst during the depolarization, while the rates of C_m creep seen in the interval between stimuli tracked the intensity of the inter-depolarization QRE bursts. For example, the first depolarization, evoking a very small C_m step and no detectable C_m creep, produced only two detectable QREs during the depolarization and none thereafter, while succeeding depolarizations producing larger steps and increasing rates of C_m creep produced bursts of QREs of increasing intensity and duration. The graph on the right, averaging 3 successive stimulus trains delivered at intervals of 100 s, demonstrates that, when appropriately scaled, the time course of charge transfer (running integral of oxidation current represented by the QREs) is nearly superposable on the time course C_m increase. This suggests that the QREs liberating 5-HT account for the majority of the C_m increase observed simultaneously. It also emphasizes the usefulness of serotonin amperometry as a single cell assay for β-cell exocytosis, in spite of evidence that 5-HT loading greatly reduces the metabolic and secretory responses of islets to glucose stimulation.[30]

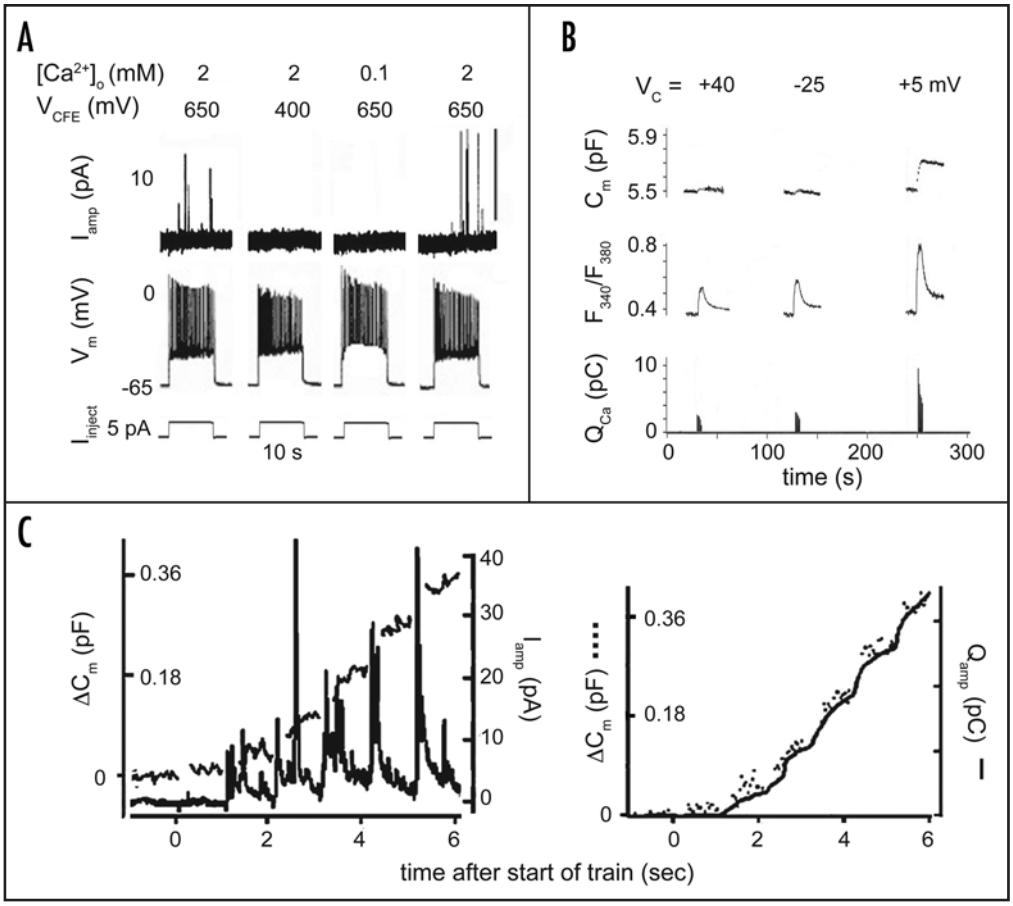

Figure 2. Single cell perforated-patch recording of depolarization-exocytosis coupling in porcine β-cells. (A) combined current clamp (V_m) and amperometry (I_{amp}) demonstrating the requirement of adequate $[Ca^{2+}]_o$ (2 vs. 0.1 mM) for exocytosis, as well as the requirement of appropriate holding voltage of the carbon fiber electrode (V_{cfe}) (+650 vs. 400 mV) for detection of individual quantal release events (QREs). (B) combined voltage-clamp, cytosolic Ca^{2+} imaging and membrane capacitance tracking, during and after trains of five 200 ms long depolarization applied at 1 Hz to different V_cs. It shows the voltage dependence of calcium entry (Q_{Ca}), the accompanying rises in cytosolic Ca^{2+} concentration ($F_{340}/F3_{800}$) and the resultant exocytosis (increase in C_m). Note the small increases in C_m on depolarization to either V_c = -25 and +40 mV, where Q_{Ca} and $F_{340}/F3_{800}$ are small, as compared with the major increase in C_m on depolarization to V_c = +5 mV, where Q_{Ca} and $F_{340}/F3_{800}$ increases are maximal. (C) comparison of time courses of exocytosis simultaneously monitored by amperometry and capacitance tracking in response to a train of six 200 ms pulses to +10 mV. Left, overlay of simultaneously recorded C_m and I_{amp} traces. Right, overlay of C_m and scaled running integral of I_{amp}. Note the closeness of overlay when a depolarization evokes either (i) a C_m step immediately after cessation of depolarizing pulse or (ii) a C_m step followed by C_m creep that persists through the interpulse interval.

Cell-to-cell heterogeneity of stimulus-depolarization and depolarization-exocytosis coupling in porcine β-cells. Cell-to-cell heterogeneity in response to low levels of nutrient stimulation (glucose <8 mM) has been well described in isolated β-cells; in single rodent β-cells this has been studied by measurement of their redox state (NAD(P)H levels), glucose phosphorylation and whole-cell K^+_{ATP} currents, and whole cell electrical activity.[10,12,31] In our examination of glucose-induced closure of K^+_{ATP} channels, cell depolarization and electrical activity in human β-cells we noted cell-to-cell heterogeneity of electrical responsiveness of even larger magnitude than previously reported in the rodent, with some cells requiring up to 15 mM glucose to trigger electrical activity.[7] To examine heterogeneity of response of porcine β-cells, we used three different cell response assays (see Fig. 3).

Initially we used a simple screening assay to examine the output of the entire cascade from glucose metabolism to Ca^{2+} entry, as

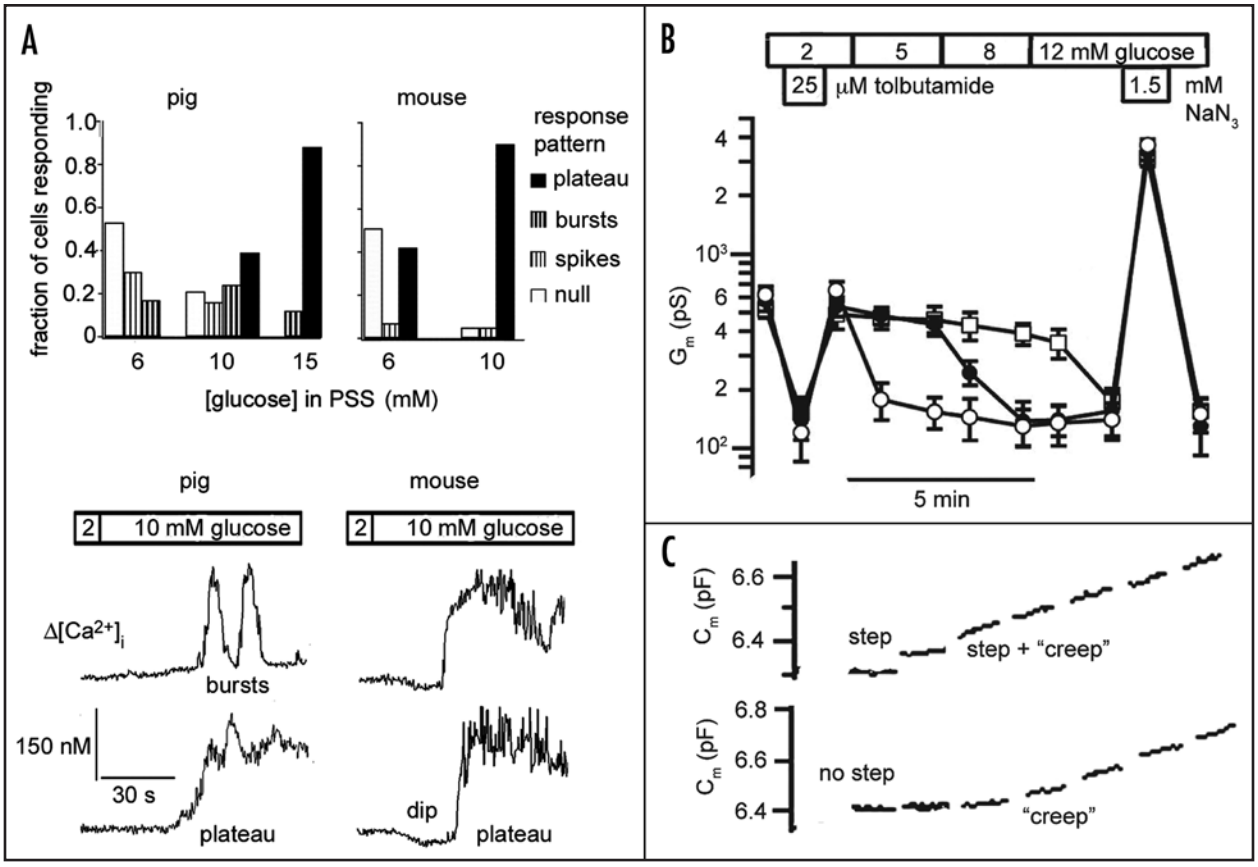

Figure 3. Cell-to-cell heterogeneity of glucose responsiveness of single porcine β-cells as assayed by glucose-induced rises in cytosolic Ca^{2+}, glucose-induced decreases in membrane conductance and depolarization induced increases in membrane capacitance. (A) heterogeneity of $\Delta[Ca^{2+}]_i$ response patterns (null response vs. spikes vs. burst vs. plateau) of 53 pig β-cells vs. 27 mouse β-cells to increases in $[glucose]_o$ from 2 to 6, 10 mM or 15 mM. Traces are typical of observed response pattern. Dip prior to plateau is typical of mouse islet β-cell. (B) summary of the glucose responsiveness of β-cell membrane conductance (G_m) in three distinct groups of β-cell recorded from using whole-cell mode. Though all cells showed nearly equal decreases in G_m to the addition of the sulfonylurea tolbutamide in the presence of low $[glucose]_o$ (=2 mM) as well as nearly equal increases in G_m to the addition of the metabolic inhibitor NaN_3 in the presence of elevated $[glucose]_o$ (=12 mM), responses to intermediate $[glucose]_o$ were highly variable. (C) showing two distinct temporal patterns of exocytosis, as assayed by increases in C_m, in response to trains of seven X 200 ms depolarizations to V_c = 0 mV at 1 Hz. In the *upper trace*, the first depolarization is followed by a step of C_m, the second is followed by an initial step of C_m and a subsequent creep of C_m, while the remaining depolarizations are followed by only creeps in C_m. In the *lower trace*, the initial depolarization evokes no detectable C_m increase while subsequent depolarizations evoke creeps in C_m of increasing slope.

displayed by Ca^{2+} indicator (Fura-2)-loaded cells exposed to a moderate secretagogue concentration of extracellular glucose. In Panel A, note the broad heterogeneity of fluorescence response of Fura-2-loaded porcine β-cells to a physiological range of glucose concentrations, as compared with the response of murine β-cells, now a standard preparation due to the growing number of experiments with transgenically generated variations.[32,33] In the presence of 6 mM glucose both species display heterogeneity of response pattern. However, in 10 mM glucose murine β-cells uniformly responded with the rapid development of a broad plateau of cytosolic $[Ca^{2+}]$, corresponding to overlapping burst-like rises in cytosolic cytosolic $[Ca^{2+}]$ (unreported data obtained in a previous study performed under similar conditions and now reanalyzed[18]), as compared with porcine β-cells, which continued to display heterogeneity of response pattern. In the porcine β-cells, near uniformity of plateau response required that bath glucose be raised to 15 mM.

Panel B displays the electrical heterogeneity of porcine β-cells in a set of perforated-patch whole-cell experiments where we continuously recorded V_m and electrical activity and intermittently probed G_m as a function of time in progressively increasing $[glucose]_o$. Note that while all cells eventually depolarized, reduced their background G_m and displayed vigorous action potential activity, at one end of the spectrum, three cells rapidly responded to 5 mM glucose while at the other end of the spectrum two cells first responded only after 3 min exposure to 12 mM glucose. In contrast, tight consistency was seen in responses to two bracketing pharmacological agents that regulate K^+_{ATP} channels activity independently of glucose metabolism. These agents are (i) tolbutamide, a sulfonylurea that at a concentration of 25 μM closes the vast majority of K^+_{ATP} channels by specifically binding to high affinity sites of the SUR1 subunits of K^+_{ATP} channels, even in the presence of high cytosolic [ATP]/[ADP], and (ii) sodium azide (NaN_3), a binder of mitochondrial cytochrome a_3, which at a concentration of

1.5 mM greatly reduces cytosolic [ATP]/[ADP] and nearly maximally opens K^+_{ATP} channels. In all cells, tolbutamide produced a nearly uniform reduction of G_m to 150 to 180 pS in the presence of 2 mM glucose, while NaN_3 produced a nearly uniform increase in G_m to 3,500 to 4,000 pS in the presence of 12 mM glucose. This suggests that the heterogeneity of glucose responsiveness was unlikely to be associated with cell-to-cell differences in the total number of activatable K^+_{ATP} channels or distinct K^+_{ATP} channel subtypes, but rather cell-to-cell differences in generation of ATP in response to glucose exposure.

Panel C displays porcine cells exocytotic heterogeneity, namely two distinct temporal patterns of exocytosis, as assayed by increases in C_m, in response to trains of seven 200 ms depolarizations to V_c = 0 mV applied at 1 Hz. In the *upper trace*, the first depolarization is followed by a step of C_m, the second by an initial step of C_m and a subsequent creep of C_m and the remaining depolarizations by only creeps in C_m. In the *lower trace*, the initial depolarization evokes no detectable C_m increase while subsequent depolarizations evoke creeps in C_m of increasing slope. These patterns will be discussed in more detail in the companion publication.

Dependence of stimulus-secretion coupling on adequate cytosolic [cAMP]. Enhancement of cytosolic concentration of cAMP is critical in augmenting glucose-induced insulin secretion in rodents and humans; moreover, it is essential "permitter" of glucose-induced insulin secretion in the dog.[28] Enhancement of $[cAMP]_i$ can be achieved by (i) direct application of membrane permeant analogs of cAMP *or* stimulators of protein kinase A (PKA), (ii) the paracrine hormone glucagon or (iii) the incretin (glucagon/secretin-like) hormones, such as glucagon-like peptide 1 (GLP-1) and glucose-dependent insulinotropic peptide (GIP), which secreted by enterochromaffin cells of the gut mucosa (reviewed in ref. 34). Likely, incretin hormones account for the large differential enhancement in insulin secretion when a load of insulin is given orally, as compared with when the same load of glucose is given intravenously. In all species investigated, enhancement of $[cAMP]_i$ appears to have at least two effects: (i) hastening of onset and augmentation of intensity of glucose-induced membrane depolarization and electrical activity[13,35] and (ii) augmentation of depolarization-exocytosis coupling, often in the absence of enhancement of Ca^{2+} entry.[36-38] As is the case with canine islets, porcine islets are very poor insulin secretors in the absence of enhancement of $[cAMP]_i$.[17] We have confirmed this finding by islet perifusion studies (see Supplementary Fig. 1) and have investigated its mechanism in single porcine β-cells.

Figure 4, panels A and B present sample data confirming in pig β-cells that addition to the bath of membrane permeable cAMP analog 8-CPT-cAMP has both proximal and distal effects on stimulus-secretion coupling. Note in *A* that addition of 200 μM 8-CPT-cAMP depolarized background V_m by 7 mV (average 7.5 mV in 4 cells), decreased G_m by 30% (average 33% in four cells), and increased AP frequency by more than 3-fold (average 2.8-fold in four cells). Note in *B* that addition of 200 μM 8-CPT-cAMP enhanced the C_m increase in response to repetitive depolarization by nearly 3-fold (average 3.2-fold in 5 cells). In the latter situation there was little change in depolarization-induced Ca^{2+} entry suggesting that the effect of the cAMP is on the efficiency of exocytosis provoked by fixed Ca^{2+} entry.

Panels *C* and *D* show, in a quantitative fashion, the exocytosis-promoting effects of cAMP enhancement by the cAMP analog as well as by the protein kinase A stimulator, forskolin and demonstrate that the hormones glucagon and GLP-1 produce similar changes in a cAMP-dependent fashion. In a series of 6 cells, where little increase in C_m was seen with repetitive depolarization in the absence of $cAMP_i$ enhancers, addition of the membrane permeant cAMP analog, 8-CPT-cAMP (at 200 μM) resulted, on average, in a 3.5-fold enhancement of total ΔC_m evoked by train of five 200 ms depolarizations to 0 mV. Similarly, the addition of forskolin (at 10 μM) resulted on average in a 2.5-fold increase total ΔC_m. Both effects were largely reversed on removal of the $cAMP_i$-enhancing agent from the bath. Subsequent or de novo addition of glucagon (at 100 nM) or GLP-1 (7–37) amide (at 10 nM) resulted in 2.5-fold and 3.5-fold enhancements, respectively, in total C_m increases evoked by train. These enhancements were largely reversed by further addition of R_p-cAMPs, a membrane permeant inhibitor of the binding of cAMP to target cAMP binding proteins.

Discussion

Porcine islets have become an increasingly important focus of new approaches to research into pathogenesis and treatment of human diabetes mellitus. First, genetically altered pigs are being developed as models of human diabetes mellitus.[1,2] Second, islets from a variety of pig sources are being developed for xenotransplantation trials for the treatment of diabetes.[3,4] These developments are not surprising given the pig's size and lifespan, as well as the similarity of its insulin to human, the latter featuring having made porcine insulin a standard treatment for insulin dependent diabetes, with few side effects, for decades before the development of human recombinant insulin. Hence, it would be highly advantageous to investigate the basic physiology of normal porcine β-cells and understand how closely they resemble normal human β-cells in their function.

From another point of view, investigation of porcine islets function is important in understanding human islet function as well. To date our understanding of human β-cells themselves is far from straightforward in that sources of human islet tissue are not truly normal pancreases but rather those harvested from either life-preserved cadavers, under ischemic conditions, or from tumor-ridden donors at the time of surgery. Early studies with these tissues suggested that human β-cells function in subtly different ways from β-cells, rapidly harvested from normal, active rodents (mice or rats). For example, human β-cells display wider heterogeneity of both the dose-response in glucose-induced closure of K^+_{ATP} channels and the time course of exocytotic response to repetitive depolarization than those seen in rodent β-cells.[6-8] In addition, human β-cells, thus far examined, routinely deploy voltage-dependent Na^+ channels and low threshold, rapidly inactivating (T-type) - Ca^{2+} channels, in addition to high threshold voltage, slowly inactivating Ca^{2+} channels, in their electrical activity,[6,9,23] as well as require some enhancement of cytosolic

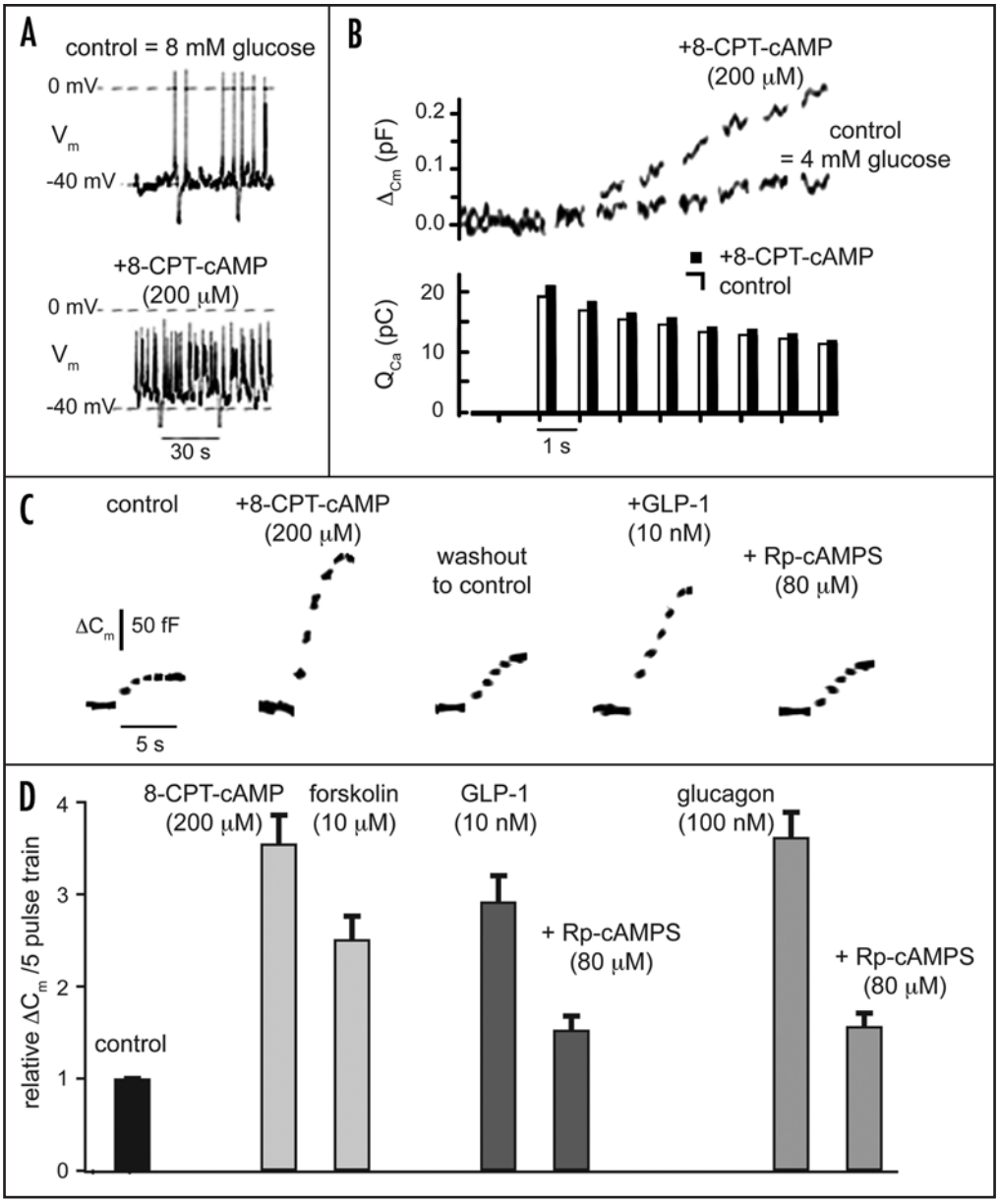

Figure 4. Dependence and modulation of glucose-induced depolarization/electrical activity and depolarization-exocytosis coupling on enhancement of cytosolic [cAMP], $[cAMP]_i$. (A) presents current clamp recording showing that after addition of 8 CPT-cAMP to a PSS containing 8 mM glucose depolarization was increased by 7 mV, background membrane conductance was reduced by 30% and the frequency of action potential activity was increased by nearly 3-fold. (B) presents voltage-clamp recording showing nearly 3-fold enhancement of depolarization-induced C_m increases after addition of 8-CPT-cAMP to a PSS containing 4 mM glucose, in spite of little to no augmentation of voltage-dependent Ca^{2+} entry (Q_{Ca}). (C) presents sample depolarization-induced C_m changes in a single cell after modulation of $[cAMP]_i$ by (i) initial addition to the bath, followed by later washout, of 8-CPT-cAMP and (ii) exposure to GLP-1 followed by inhibition of its action, by further addition to the bath of R_p-cAMPS. (D) presents a graphical summary of effects of $[cAMP]_i$-altering maneuvers in a set of 6 cells. Note the qualitatively similar effects of membrane permeable cAMP analog (8-CPT-cAMP), PKA activator (forskolin), the incretin GLP-1 and the paracrine hormone glucagon. Note partial reversal of the effects of both GLP-1 and glucagon by R_p-cAMPS.

of islets obtained from brain-dead donors.

In this first detailed report on the electrophysiology of stimulus-exocytosis coupling in porcine β-cells, we demonstrate that β-cells derived from freshly obtained pancreati preserve three traits prominently displayed by human β-cells. These are as follows: (i) the routine use of voltage dependent Na^+ channels in excitability, (ii) the broad heterogeneity of glucose-induced closure of K^+_{ATP} channels; and (iii) heterogeneity of time course of exocytosis in response to repetitive depolarization as measured by the single cell assays of capacitance and amperometry. This suggests that the later distinguishing features may be intrinsic to stimulus-exocytosis coupling in larger, long-lived mammals. Furthermore, we confirm the finding that porcine islets, like many human islets, require conditions that enhance cytosolic [cAMP] in order to potently secrete insulin as well as provide *two mechanistic bases*, in single β-cells, for the finding, namely the potentiation of both glucose-induced cell depolarization and depolarization-induced exocytosis in the face of sizeable Ca^{2+} currents and resultant increases in cytosolic $[Ca^{2+}]$. While these studies demonstrate a clear protein kinase A-dependent component of cAMP action, they do not rule out or quantitative dissect out the contribution of a component attributable to cAMP-regulated guanine nucleotide exchanger factors (cAMPGEF or Epac), in that the cAMP analog we used activated both pathways and R_p-cAMPs is a poor blocker of Epac. Lastly, it is worth noting that on the basis of work in other species, here we chose for study, as presumed β-cells, isolated islet cells >12 μm in diameter and baseline capacitance of >5.5 pF. This working hypothesis was supported by results from our limited recordings from cells <10 μm in diameter and with baseline capacitance of <4.5 pF. The latter cells showed action potential activity

[cAMP] to exhibit potent first phase insulin secretion and recognizable second phase insulin secretion.[6,8] Currently, it is uncertain whether these differentiating features are intrinsic to human β-cells in situ, or a function of the metabolically "stunned" state of islets

at 2–3 mM glucose, rapid development of plateau depolarization at 8–12 mM glucose (5/5 cells), and exclusively T-type Ca^{2+} (4/4 cells), features all characteristic of α-cells in other mammalian species.[40]

In the case of voltage-dependent channels used for electrical activity, we suggest that glucose-induced depolarization brings V_m towards -45 to -40 mV where the opening of a small number of the ample complement of Na^+ channels, which is only 50% inactivated, is sufficient to trigger an action potential, without resort to low threshold T-type Ca^{2+} channels prevalent in human but undetectable in pig. The vigorously activating Na^+ currents account the fast upstroke and overshoot of the majority of the APs thereby rapidly bringing V_m into a range where slowly inactivating high voltage activated (HVA) Ca^{2+} channels are opened and underlie depolarization evoked exocytosis. Our single channel recordings and pharmacological trials suggest that the HVA Ca^{2+} channels are of the L-type variety, though we did not probe them for conotoxin sensitivity to rule out P/Q or R types, as recently reported in human β-cells.[9] Action potential repolarization results from the slower voltage-dependent activation of slowly inactivating delayed rectifier type K^+ channels, as well as (i) Ca^{2+} entry-dependent activation of Ca^{2+} activated K^+ channels, likely of the SK variety (see Supplementary Fig. 2), though the single channel analysis and detailed pharmacology of the latter currents was not undertaken and, in the occasional cell, (ii) a small component of rapidly inactivating A-type voltage dependent K^+ channels (data not presented here).[41]

In the case of heterogeneity of cell response, we present evidence that the heterogeneity of glucose-induced closure of K^+_{ATP} channels appears to be due to the heterogeneity of glucose importation or metabolism rather than intrinsic heterogeneity of [ATP]/[ADP] sensitivity of K^+_{ATP} channels. In cells with widely differing glucose responsiveness, whole-cell membrane conductance (G_m) displays a rather uniformly *decrease* in response to a dose of tolbutamide, which closes the majority of highly sulfonyurea sensitive (SUR 1 + Kir 6.2) K^+_{ATP} channels, as well as a rather uniform *increase* in response to a dose of metabolic inhibitor NaN_3 that decreases cytosolic [ATP]/[ADP]. In addition, in pilot experiments, single K^+_{ATP} channel activity in inside-out excised membrane patches display rather uniform sensitivity to alterations in [ATP] and [ADP], even though prior to patch excision the same K^+_{ATP} channels, in the cell attached patch configuration, displayed widely variant glucose-responsive closure (see Supplementary Fig. 3).

However, of the two major features of cell-to-cell heterogeneity noted, we would argue that the heterogeneity of temporal pattern of exocytosis may be more important physiologically. In situ, the electrical coupling of β-cells within the intact islet by gap junctions should synchronize electrical activity in cells that in isolation display differential glucose-induced closure of K^+_{ATP} channels, and therefore limit the importance of the disparity. In contrast, the same electrical coupling is likely to augment the importance of depolarization-induced heterogeneity of exocytosis by insuring widespread depolarization of cells. We have examined in more detail the heterogeneity of exocytotic patterns, the enhancement of these patterns by the augmentation of cytosolic [cAMP] in a companion paper. There, in addition, we consider the implications of this heterogeneity for sustaining long term depolarization-exocytosis coupling in the face of changing patterns of electrical activity (e.g., transition from volleys of action potentials to plateau depolarizations) sometimes seen in β-cells.

Methods

Preparation of islets and single islet cells. Porcine islet tissue was generously provided by the Islet Transplantation Laboratory of the Diabetes Research and Training Center of Washington University Medical Center. Pancreata, harvested at the local slaughterhouse during the process of deguttation, were digested with collagenase. Thereafter, islets were separated on a Ficoll gradient using protocols nearly identical to those developed for human tissue.[15] The resultant islet tissue was handled in a manner nearly identical to that we have described for human islet isolates.[8,16] That is, islet tissue was cultured in CMRL for 1–2 days at 37°C in a 5% CO_2 + 95% air environment or for up to 10 days at room temperature and then for 1 to 3 days at 37°C in the 5% CO_2 + 95% air environment prior to use. Subsequently, islet tissue was dispersed to single cells using either of two methods. (i) In the presence of gentle stirring, tissue was enzymatically dispersed by incubation for 1–3 min in Versene 1:5,000 (Gibco BRL, Grand Island, NY), followed by exposure to dispase (0.33 mg/ml, Boehringer Mannheim GmbH, Germany), (ii) Tissue was mechanically dispersed by brief incubation at 30°C in trypsin-EDTA 1X (Sigma, St. Louis, MO) accompanied by trituration. While in situ both human and porcine islets are oval or oblong, the islet tissue harvested from pigs consisted of strands or clumps of islet cells rather than discrete oval or oblong islets seen with human islet isolates.[15] However, fixed, thin sections of tissue of both tissues examined under the electron microscope consisted almost exclusively of cells with dense core secretory granules 200–300 nm in diameter and in nearly 70% of cells, granules with central rectangular crystals, characteristic of insulin condensed with Zn^{2+}, were seen.

The results of two sets of preliminary experiment insured that our tissue was metabolically active and secretion-competent. *First*, when islets were perifused with an oxygenated, well-buffered Kreb's solution. in the presence of either 0.25 mM isobutylmethylxanthine (IBMX), a non-selective phosphodiesterase inhibitor or 10åμM forskolin, a direct activator of protein kinase A, insulin secretion, assessed by radioimmunoassay, was vigorously biphasic (rapid spike + prolonged plateau) in response to a rise in glucose from 2 to 12 mM (see Supplementary Fig. 1). Both phases of secretion were reduced by at least 70% (i) by transient reduction of perifusate [Ca^{2+}] from 2 to 0.2 mM, consistent with Ca^{2+} entry requirement for electrical activity and rinsulin granule exocytosis; or (ii) by addition to the bath of a small concentration of the mitochondrial blocker sodium azide (NaN_3), consistent with the need for oxidative metabolism of glucose as a trigger for glucose-induced insulin release. Consistent with a recent report,[11] similar reductions in both phases of secretion were also seen in the absence of either IBMX or forskolin, thereby demonstrating the dependence of adequate secretion on the presence of a cAMP enhancing agent. *Second*, when incubated with ^{14}C-labelled glucose, dispersed

islet tissue demonstrated a 4-fold increase in the production of ^{14}C-labelled CO_2 in the presence of 12 vs. 3 mM glucose.

Single cell recording of ion currents, electrical activity, cytosolic [Ca^{2+}] and insulin granule exocytosis. Single cell electrical and electrochemical recording, as well as fluorescence measurement of cytosolic calcium, were performed 2 to 7 days after islet dispersion, using patch clamp, Ca^{2+} imaging, capacitance tracking and amperometry techniques were nearly identical to those we have previously used on human β-cells.[8,14,16] The single islet cells selected for in this study were >12 μm in diameter and had a baseline capacitance of >5.5 pF, criteria previously used to identify β-cells in other species.[18,19] The standard physiological saline solution (PSS) bath contained in mM: 137.5 NaCl; 5.5 KCl; 2 $CaCl_2$; 0.1 $MgCl_2$; 2 glucose, and 20 HEPES titrated to pH 7.35 with NaOH; it was maintained at 32°C to simulate near physiological temperature. Solutions were modified by isosmotic replacement of a portion of the NaCl content with a pharmacological agent (e.g., NaCl with tetraethylammonium (TEA) chloride to facilitate recording of Ca^{2+} currents in isolation). In the case of perforated-patch recording used for whole-cell voltage (or current) or monitoring, patch pipettes were filled with a high K^+ (or high Cs^+) internal solution, designated K^+-IS (or Cs^+-IS). These contained, in mM: 63.7 KCl (or CsCl); 28.35 K_2SO4 (or Cs_2SO_4); 47.2 sucrose; 11.8 NaCl; $MgCl_2$; 0.5 mM EGTA and 20 HEPES titrated to pH 7.35 with KOH (or NaOH). Nystatin (200–250 μg/ml) was added to the 2–5 μl volume of solution just proximal to the tip of the pipette to permit perforated-patch whole-cell recording using a Heka EPC-9 patch clamp amplifier (Instrutech, Corp., Great Neck, NY). Whole cell current clamp recording was begun once pipette-to-cytoplasm access resistance (R_a) fell to <40 MΩ, while voltage-clamp recording was begun after R_a fell to <30 to 25 MΩ. Whole-cell currents were leak subtracted using a standard p/4 protocol.

Free cytosolic Ca^{2+} concentration, $[Ca^{2+}]_i$, was estimated from ratiometric measurements (photon counting of fluorescence emission at 510 nm after dual wavelength excitation at 340 and 380 nm) made on cells loaded with membrane permeant, acetoxymethylester (AM) derivative of Fura-2 (Molecular Probes, OR),[8,16] using an Olympus IX inverted fluorescence microscope and T.I.L.L. Photonics Imaging System II (Polychrome II excitation spectrophotometer, an intensified CCD camera, and TILLvisION software (Applied Scientific Instrumentation, Inc., Eugene, OR). Ratiometric data was converted to a running estimate of $[Ca^{2+}]_i$ using a standard equation,

$$[Ca^{2+}]_i = K_d\ (R - R_{min})/(R_{max} - R) * (F_{380,max}/F_{380,min}),$$

where K_d = 224 nM, and R_{max} and $F_{380,max}$ and R_{min} and $F_{380,min}$ were obtained sequentially after adding 5 μM ionomycin and then at least 5 mM EGTA to the bath.[20]

Quantal release events (QREs) were monitored by amperometry using a carbon fiber electrode (tip potential = +650 mV) positioned at the surface of a cell (i) previously loaded with serotonin (5-HT) and 5-hydroxytryptophan, at incubation concentrations of 0.5 mM each, and then (ii) bathed in a PSS containing 4 mM glucose and 10 μM forskolin.[8,21] Membrane capacitance changes (ΔC_m) following cell depolarization were estimated using an EPC-9 patch clamp amplifier (Heka, Electronic, Lambrecht, Germany) and software-based, dual frequency lock-in detector (LID) developed as a set of extensions (XOP modules) of the numerical/graphics package Igor (Wavemetrics, Inc., Oregon, USA) designed to (i) apply dual-frequency, small signal voltage excitation (10 mV peak-to-peak at 400 and 800 Hz) to the cell held at a DC potential of -70 mV and then (ii) process the current response.[22]

Salts, small organic molecules, and peptides (glucagon and glucagon-like peptide-1 (9–37) amide) were purchased from Sigma-Aldrich Chemicals (St. Louis, MO).

Acknowledgements

We thank (i) Human Islet Transplantation Laboratory, Washington University Medical Center, and especially Barbara Olack and Carole Swanson, for the provision of islets; (ii) Sarah Boyle, Connie Marshall and Robert Henry for help with tissue characterization (islet perifusions shown in Supplementary Figure 1, islet glucose oxidation and islet ultrastructure, respectively); and (iii) Alon Friedman, Advanced Teacher Training Center at Shlomi, Israel for expert help with design and execution of several of the figures. This work was principally supported by grants from the National Institutes of Health: 4RO1-DK37380 to Stanley Misler and ROI-DK20579 to M. Mohanakumar (Dept. of Surgery, Washington University in St. Louis) for isolation of islets. Additionally, Amelia M. Silva was partially supported by a grant from the Luso-American Foundation of Portugal and Adam S. Dickey was supported by a National Institutes of Health Medical Scientist Training Grant (5T32 GM07281) to the University of Chicago.

Note

Supplementary materials can be found at:
www.landesbioscience.com/supplement/SilvaCHAN3-2-Sup.pdf

References

1. Larsen MO, Wilken M, Gotfredsen CF, Carr RD, Svendsen O, Rolin B. Mild streptozotocin diabetes in the Göttingen minipig, a novel model of moderate insulin deficiency and diabetes. Am J Physiol Endocrinol Metab 2002; 282:26-7.
2. Korte FS, Mokelke EA, Sturek M, McDonald KS. Exercise improves impaired ventricular function and alterations of cardiac myofibrillar proteins in diabetic dyslipidemic pigs. J Appl Physiol 2005; 98:461-7.
3. Korsgren O, Buhler LH, Groth CG. Toward clinical trials of islet xenotransplantation. Xenotransplantation 2003; 10:289-92.
4. Hering BJ, Wijkstrom M, Graham ML, Hårdstedt M, Aasheim TC, Jie T, Ansite JD. Prolonged diabetes reversal after intraportal xenotransplantation of wild-type porcine islets in immunosuppressed nonhuman primates. Nat Med 2006; 12:301-3.
5. Ashcroft FM, Rorsman P. Electrophysiology of pancreatic beta cells. Prog Biophys Mol Biol 1991; 54:87-143.
6. Misler S, Barnett DW, Gillis KD, Pressel DM. Electrophysiology of stimulus-secretion coupling in human β-cells. Diabetes 1992; 41:1221-8.
7. Misler S, Pressel DM, Gillis KD. Depolarization-secretion coupling in pancreatic β-cells: do diverse excitability patterns support insulin secretion? In Proc 14th Congress Int Diabetes Fed, Elsevier, Amsterdam 1991; 361-5.
8. Misler S, Dickey A, Barnett DW. Maintenance of stimulus-secretion coupling and single beta-cell function in cryopreserved-thawed human islets of Langerhans. Pfluegers Arch 2005; 450:395-404.
9. Braun M, Ramracheya R, Bengtsson M, Zhang Q, Karanauskaite J, Partridge C, et al. Voltage-gated ion channels in human pancreatic beta-cells: electrophysiological characterization and role in insulin secretion. Diabetes 2008; 57:1618-28.

10. Heimberg H, De Vos A, Vandercammen A, Van Schaftingen E, Pipeleers D, Schuit F. Heterogeneity in glucose sensitivity among pancreatic beta-cells is correlated to differences in glucose phosphorylation rather than glucose transport. EMBO J 1993; 12:2873-9.
11. Vidaltamayo R, Sanchez-Soto MC, Hiriart M. Nerve growth factor increases sodium channel expression in pancreatic β cells: implications for insulin secretion. FASEB J 2002; 16:891-2.
12. Kinard TA, deVries G, Sherman A and Satin LS. Modulation of the bursting properties of single mouse pancreatic b-cells by artificial conductances. Biophysical J 1999; 76:1423-35.
13. Barnett DW, Pressel DM, Chern HT, Scharp DW, Misler S. cAMP-enhancing agents "permit" stimulus-secretion coupling in canine pancreatic islet beta-cells. J Membrane Biol 1994; 138:113-20.
14. Pressel DM, Misler S. Role of voltage dependent ionic currents in coupling glucose stimulation to insulin secretion in canine pancreatic islet β-cells. J Membrane Biol 1991; 124:239-53.
15. Swanson CJ, Olack BJ, Goodnight D, Zhang L, Mohanakumar T. Improved methods for the isolation and purification of porcine islets. Human Immunology 2001; 62:739-49.
16. Silva AM, Liu-Gentry J, Dickey AS, Barnett DW, Misler S. α-Latrotoxin increases spontaneous and depolarization-evoked exocytosis from pancreatic islet β-cells. J Physiol 2005; 565:783-99.
17. Dufrane D, Nenquin M, Henquin JC. Nutrient control of insulin secretion in perifused adult pig islets. Diabetes Metab 2007; 33:430-8.
18. Pipeleers D and Van der Winkel M. Separation of pancreatic islet cells according to functional characteristics. In *Cell Separation: Methods and Selected Applications*, Pertlow TG, Academic Press, Orlando 1987; 119-40.
19. Göpel S, Kanno T, Barg S, Galvanovskis J, Rorsman P. Voltage-gated and resting membrane currents recorded from β-cells in intact mouse pancreatic islets. J Physiol 1999; 521:717-28.
20. Grynkiewicz G, Poenie M, Tsien RY. A new generation of Ca^{2+} indicators with greatly improved fluorescence properties. J Biol Chem 1985; 260:3440-50.
21. Zhou Z, Misler S. Amperometric detection of quantal secretion from patch-clamped rat pancreatic beta-cells. J Biol Chem 1996; 271:270-7.
22. Barnett DW, Misler S. An optimized approach to membrane capacitance estimation using dual-frequency excitation. Biophys J 1997; 72:1641-58.
23. Barnett DW, Pressel DM, Misler S. Voltage-dependent Na^+ and Ca^{2+} currents in human pancreatic islet beta-cells: evidence for roles in the generation of action potentials and insulin secretion. Pfluegers Arch 1995; 431:272-82.
24. Gillis K, Misler S. Single cell assays of exocytosis from pancreatic B-cells. Pfluegers Arch 1992; 420:121-3.
25. Ammala C, Eliasson L, Bokvist K, Larsson O, Ashcroft FM, Rorsman P. Exocytosis elicited by action potentials and calcium currents in individual mouse pancreatic B-cells. J Physiol 1993; 472:665-88.
26. Smith PA, Duchen MR, Ashcroft FM. A fluorimetric and amperometric study of calcium and secretion in isolated mouse pancreatic beta-cells. Pfluegers Arch 1995; 430:808-18.
27. Huang L, Shen H, Atkinson MA, Kennedy RT. Detection of exocytosis from individual pancreatic beta cells by amperometry at a chemically modified microelectrode. Proc Natl Acad Sci USA 1995; 92:9608-218.
28. Bruns D, Jahn R. Real-time measurement of transmitter release from single synaptic vesicles. Nature 1996; 377:62-5.
29. Zhou Z, Misler S. Amperometric detection of stimulus-induced quantal release of catecholamines from cultured superior cervical ganglion neurons. Proc Natl Acad Sci USA 1995; 92:6938-42.
30. Zawalich WA, Tesz GJ, Zawalich KC. Are 5-hydroxytrptamine-preloaded b-cells an appropriate physiological model for establishing that insulin stimulates insulin secretion? J Biol Chem 2001; 276:37120-3.
31. Rochelleau JV, Remedi MS, Granada B, Head WS, Koster JS, Nichols CG, Piston DW. Critical role of gap junction coupled K_{ATP} channel activity for regulated insulin secretion. PloS Biology 2006; 4:221-7.
32. Ashcroft FM. ATP-sensitive potassium channelopathies: focus on insulin secretion J Clin Invest 2005; 115:2047-58.
33. Merrins MJ, Stuenkel EL. Kinetics of Rab27a-dependent actions on vesicle docking and priming in pancreatic beta-cells. J Physiol 2008; 586:5367-81.
34. Holst JJ. The physiology of glucagon-like peptide-1. Physiol Rev 2007; 87:1409-39.
35. Holz GG, Kuehtreiber WM, Habener JF. Pancreatic beta-cells are rendered glucose-competent by the insulinotropic hormone glucagon-like peptide-(17–37). Nature 1993; 361:362-5.
36. Ammala C, Ashcroft FM, Rorsman P. Calcium independent potentiation of insulin release by cyclic AMP in single β-cells. Nature 1993; 363:356-8.
37. Gillis KD, Misler S. Enhancers of cytosolic cAMP augment depolarization-induced exocytosis from pancreatic B-cells: evidence for effects distal to Ca^{2+} entry. Pfluegers Arch 1993; 424:195-7.
38. Gromada J, Bokvist K, Ding WG, Holst JJ, Nielsen JH, Rorsman P. Glucagon-like peptide 7–37 amide stimulated exocytosis in human pancreatic beta-cells by both proximal and distal regulatory steps in stimulus-secretion coupling. Diabetes 1998; 47:57-65.
39. Holz GG. Epac: a new cAMP binding protein in support of glucagon-like peptide-1 receptor-mediated signal transduction in the pancreatic β-cell. Diabetes 2004; 53:5-13.
40. Goepel SO, Kanno T, Barg S, Weng X-G, Gromada J, Rorsman P. Regulation of glucagon release in mouse alpha cells by KATP channels and inactivation of TTX-sensitive Na channels. J Physiol 2000; 528:509-20.
41. Kozak JA, Misler S, Logothetis DE. Characterization of a Ca^{2+}-activated K^+ current in insulin-secreting murine betaTC-3 cells. J Physiol 1998; 355-70.